Clays and Clay Minerals, Vol. 29, No. 5, 385–396, 1981.

ZEOLITE DIAGENESIS BELOW PAHUTE MESA, NEVADA TEST SITE

GEORGE K. MONCURE
Conoco Inc., Exploration Research, Ponca City, Oklahoma 74601

RONALD C. SURDAM
Department of Geology, University of Wyoming, Laramie, Wyoming 82071

H. LAWRENCE MCKAGUE
University of California, Lawrence Livermore National Laboratory, Livermore, California 94550

Abstract—The Tertiary silicic volcanic rocks in the Silent Canyon Caldera beneath Pahute Mesa, of the Department of Energy's Nevada Test Site have been divided into three vertical mineralogical zones that vary in thickness and transgress stratigraphic boundaries. Zonal contacts are generally sharp. Zone 1, the uppermost zone, includes unaltered or incipiently altered rhyolitic glass. Zone 2 is characterized by a predominance of clinoptilolite and subordinate amounts of smectite, cristobalite, and mordenite. Zone 3 is a complex mineral assemblage that includes analcime, quartz, calcite, authigenic K-feldspar and albite, kaolinite, chlorite, and mixed-layer illite/smectite. The mixed-layer clay shows an increase in ordering and a decrease in expandability with depth.

Shortly after deposition and after shallow burial, hydration of relatively impermeable, highly porous vitric rocks resulted in the rapid formation of the Zone 2 assemblage (except mordenite). This stage of alteration resulted in a net porosity loss and negligible mass transfer. Continued burial and rise in temperature led to a dehydration stage in which the Zone 2 assemblage was replaced by the Zone 3 minerals. The dehydration stage resulted in a porosity increase and an increase in permeability of several orders of magnitude. This process, like the earlier reactions, also conserved mass. Precipitation of mordenite followed the formation of this zonal configuration. The diagenetic zones below Pahute Mesa were caused by: (1) changing pore-water chemistry in an essentially closed hydrologic system; (2) disequilibrium or kinetic precipitation of metastable phases; and (3) a higher thermal gradient than that now present.

Key Words—Analcime, Clinoptilolite, Closed hydrologic system, Diagenesis, K-feldspar, Mordenite, Zeolite.

INTRODUCTION

Recently, silicate diagenesis has been the focus of many investigators due to its impact on porosity and permeability in sedimentary rocks. Zeolite diagenesis is of particular interest because of the abundance of volcanogenic sediments in the geologic record, but many problems remain unsolved because of difficulties in evaluating the thermal, chemical, and physical properties of these rocks. To compound these problems, zeolites have variable compositions and behave metastably. Few useful thermodynamic data exist on zeolites, and alternatives to traditional approaches must be developed to study their diagenesis. This investigation evaluates a geologic setting undergoing zeolite diagenesis using the following approach: (1) determination of diagenetic mineral patterns, or at least mineral distributions; (2) documentation of mineral reactions; (3) establishment of reaction mechanisms; (4) calculation of mass balance; and (5) if possible, quantification of the mass transfer, or at least its relationship to porosity and permeability.

The Tertiary silicic volcanic rocks within the Silent Canyon Caldera (Pahute Mesa, Nevada Test Site of the Department of Energy—see Figure 1) provide a natural laboratory for the study of zeolite diagenesis because of the relatively uniform chemical composition of primary materials and the moderately uncomplicated thermal and structural history. Excellent stratigraphic control, availability of core samples, and ground-water accessibility further facilitate such diagenetic studies. Detailed analysis of core from Wells UE20f, UE20h, and PM-1 (see Figure 2) yielded the primary data on which this study is based.

The Silent Canyon Caldera is an almost completely buried Late Miocene volcanic center in southern Nevada (Orkild *et al.*, 1968). Collapse of the caldera coincided with the eruption of the Belted Range Tuff (13 to 14 my). With collapse of the caldera, the Belted Range Tuff was downdropped 1.5 to 2 km into an elliptical, 30 × 42 km depression. Subsequently, the depression was filled by related tuffs and lavas, and still later, tuffs associated with the Timber Mountain (11

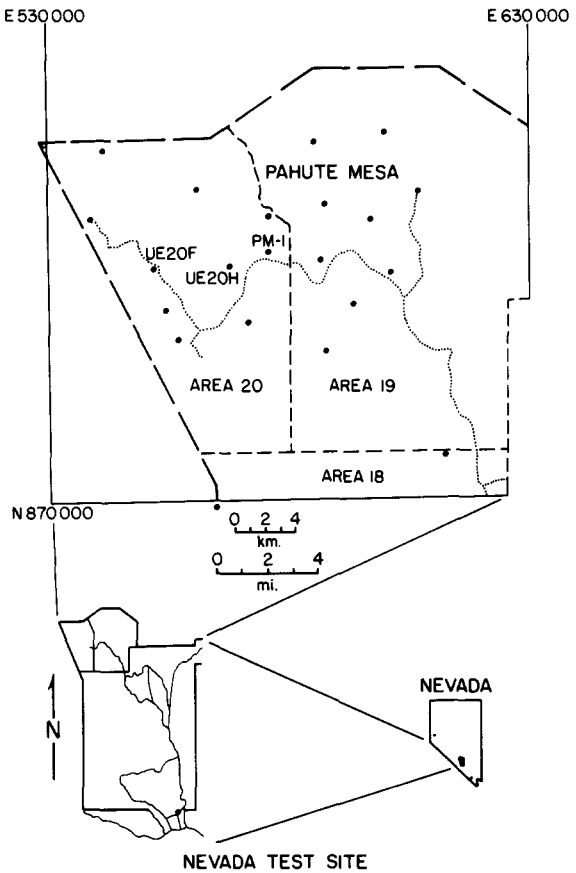

Figure 1. Location map of Pahute Mesa, Nevada Test Site. Dots represent locations of drill holes.

my) and Black Mountain (7 my) volcanic centers completely filled and nearly obscured the Silent Canyon Caldera. All samples examined in this study are from post-Belted Range tuffs and lavas.

Hay (1963) proposed an "open system" model to explain the vertical zeolite zonation in the Oligocene-Miocene John Day Formation of Oregon. With a similar open-system interpretation, Hoover (1968) briefly described the vertical zonation of authigenic phases in the Tertiary rocks of the Nevada Test Site. A summary of his study follows:

> Zeolite zoning, chemistry of the zeolitized rocks and a lack of correlation of zones with depth suggest that the zones were formed from the leaching of vitric rocks, an increase in cation content and pH with depth and a reduced ground-water flow above relatively impermeable rocks. On the basis of petrographic evidence, clay minerals formed first, followed by clinoptilolite, then mordenite and finally analcime.

The chemical, mineralogical, and textural data that follow suggest contrasting diagenetic mechanisms and a different paragenetic sequence to explain the diagenetic history of Pahute Mesa.

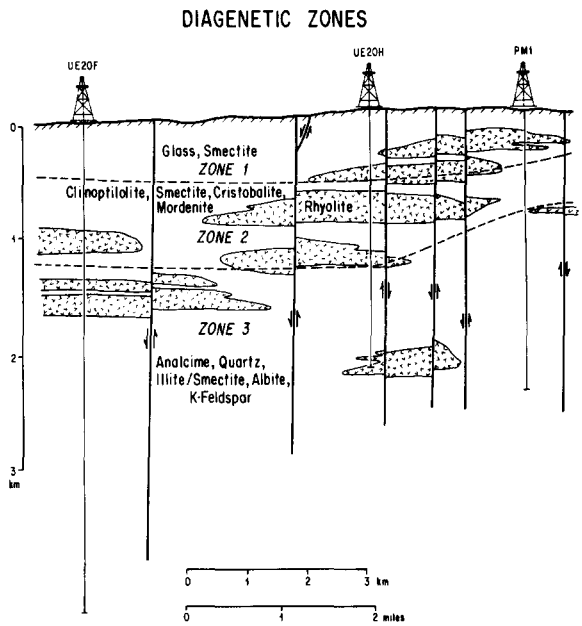

Figure 2. Schematic cross section through Wells UE20f, UE20h, and PM-1. Modified from Orkild *et al.* (1969).

ANALYTICAL METHODS

Core samples were ground to <50 μm in preparation for the following analyses:

1. Powder-pack mounts, used to produce "random" orientation, were made for bulk X-ray diffraction mineral analyses. The mounts were run at 2°2θ/min from 4° to 50°2θ (CuKα radiation).
2. For clay mineral identification, the <2-μm size fractions were obtained by centrifugation and oriented mounts were prepared using the methods of Drever (1973).
3. Bulk chemical analyses were carried out by atomic absorption spectroscopy.
4. Total carbon (by combustion-coulometric method) and inorganic carbon (hot-acid titration method) were obtained to determine the weight percent organic carbon (by difference).
5. Mineral compositions were determined with an ARL electron microprobe.

MINERALOGICAL RESULTS

The Tertiary rocks beneath Pahute Mesa may be divided into three mineralogic zones, each characterized by a particular suite of diagenetic minerals (Figure 2). Zone 1, the uppermost zone, includes unaltered to incipiently altered rhyolitic glass. Zone 2 is characterized by a predominance of clinoptilolite and subordinate

https://doi.org/10.1346/CCMN.1981.0290508 Published online by Cambridge University Press

Table 1. Partial major-element analyses of "primary" volcanic material.

Sample[1]	Oxides (wt. %)						
	SiO_2	Al_2O_3	K_2O	Na_2O	CaO	MgO	Fe_2O_3
UE20f-0.30 Devitrified vitric tuff	76.3	10.8	4.90	3.37	0.49	0.25	1.18
UE20f-0.46 Vitric tuff	74.2	10.8	4.61	3.45	0.49	0.14	1.15
UE20f-0.99[2] Rhyolite	78.3	11.8	5.1	3.0	0.64	0.08	0.91
UE20f-1.10 Vitrophyre	74.2	10.7	4.99	3.18	0.60	0.08	1.10
UE20f-1.38 Rhyolite	75.2	11.6	4.14	3.86	0.76	0.21	1.93
UE20f-1.50 Rhyolite	75.7	10.6	3.91	3.48	0.71	0.24	2.53
UE20f-2.59 Rhyolite	76.8	10.7	4.80	3.68	0.30	0.07	1.96
UE20f-2.74 Rhyolite	73.7	10.8	4.96	3.77	0.22	0.05	2.67
UE20f-2.90 Rhyolite	76.4	10.9	4.46	3.25	0.20	0.04	1.80

[1] Last three digits = depth, in km.
[2] From Quinlivan and Byers (1977). Others by Steve Boese, University of Wyoming.

amounts of smectite, cristobalite, and mordenite. Zone 3 contains a complex mineral assemblage that includes analcime, quartz, calcite, authigenic K-feldspar and albite, kaolinite, chlorite, and mixed-layed illite/smectite. These zones vary in thickness laterally and transgress stratigraphic boundaries (Hoover, 1968). Zonal contacts are generally sharp, although mineralogical elements from a shallower zone may be found well within a deeper zone. The three diagenetic zones are developed in rhyolitic pyroclastic rocks that have various amounts of quartz and feldspar phenocrysts or clasts and rhyolitic lithic fragments. Most plagioclase is zoned, having compositions that average An_{23} to An_{27}. Common accessory minerals are biotite, hornblende, apatite, and sphene.

Glass

The predominant phase in Zone 1 is volcanic glass, and based on relict glass-shard outlines in the other zones, it is the solid component from which most of the other authigenic phases were derived. The chemical compositions of unaltered glasses (Table 1) are similar to each other as well as to rhyolites regardless of sample depth beneath Pahute Mesa. Figure 3 shows the typical porous texture of unaltered glass from the upper part of Zone 1. Deeper in the same zone, incipient argillization forms rims fringing glass fragments. Still deeper, bordering Zone 2, clinoptilolite crystals have formed adjacent to smectite rims.

Clay minerals

X-ray powder diffraction (XRD) analyses indicate that the clay minerals in the cores are segregated into the different diagenetic zones. Smectite is restricted chiefly to Zones 1 and 2. Accurate microprobe analyses of the smectite were not obtainable due to the intermixing of smectite with cristobalite fibers. However, approximate cation ratios were determined, and compositions were estimated.

The clay mineral assemblage in Zone 3 is more complex than that in shallower zones. The appearance of a poorly ordered, mixed-layer illite/smectite (I/S) having a high expandability in part marks the boundary between Zone 2 and Zone 3. The mixed-layer phase shows a persistent increase in ordering and decrease in expandability with increased depth in Zone 3. The presence of discrete smectite within Zone 3 makes quantification of I/S expandability difficult. However, Figure 4 demonstrates the overall decrease in the amount of smectite relative to illite with depth in Zone 3.

Accessory clay minerals in Zone 3 include kaolinite and chlorite. In thin section, kaolinite was noted as an alteration product of plagioclase, and chlorite, predominantly as a fine-grained fracture cement.

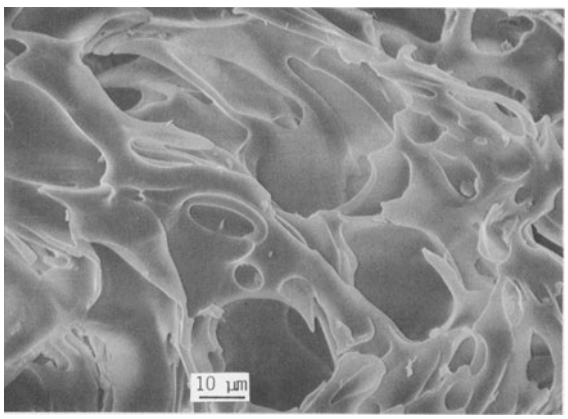

Figure 3. Scanning electron micrograph of unaltered glass from Zone 1.

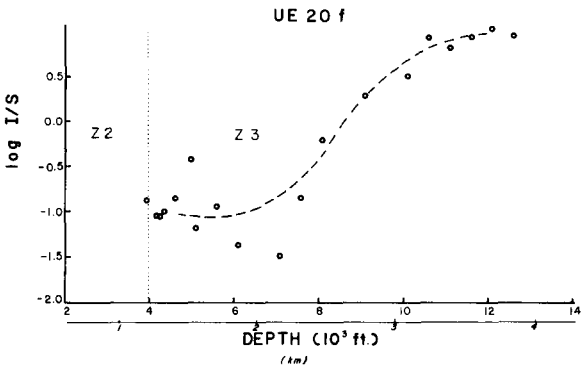

Figure 4. Plot of log I/S versus depth for Well UE20f where I = illite 002 peak area and S = smectite 001 peak area.

Clinoptilolite

Clinoptilolite is the predominant zeolite in Zone 2 (~70–90% by weight), where it commonly occurs with cristobalite, smectite, and mordenite (particularly in the lower portion of Zone 2) and less commonly with glass, authigenic K-feldspar, and analcime. In thin section or by scanning electron microscopy, clinoptilolite occurs as tabular, coffin-shaped crystals lining dissolved glass shards with the long axes of the crystals oriented perpendicular to shard margins (Figure 5). Clinoptilolite was not found occupying primary pore spaces. Partial electron microprobe analyses of four clinoptilolites are listed in Table 2.

Mordenite

Mordenite is found in Zone 2 (increasing in abundance toward the lower part of the zone) and only in the upper part of Zone 3. It occurs as fibrous masses filling pore space or as thin, scattered fibers over clinoptilolite and cristobalite inside relict shard outlines or over analcime and albite (Figure 6). Mordenite was not observed as a direct alteration product of glass. The fibers and masses of mordenite were too fine or too intimately associated with cristobalite, clays, or other zeolites to be analyzed by electron microprobe.

Analcime

Analcime occurs only in Zone 3 and decreases in abundance with depth (from 0 to 40% by weight, see Figure 2). Two forms were observed: (1) pseudomorphs after clinoptilolite within shard outlines (Figure 7), and (2) pore cements outside of relict shard outlines (Figure 8). Electron microprobe analyses of analcime from the three cores are listed in Table 3. The analcimes have high Si/Al ratios (about 2.4 to 2.7) and may be classified as "Group A" analcime as defined by Coombs and Whetten (1967).

Cristobalite

Two forms of cristobalite were recognized in the upper two zones in zeolitized and nonzeolitized rocks (Figure 2). The first type occurs in axiolitic textures intermixed with tridymite and feldspars and is clearly a result of devitrification during cooling of the rock (Ross and Smith, 1961). The second type is diagenetic in origin and is found in Zone 2 in the form of minute (~5–8 μm) spherules perched on clinoptilolite (Figure 9) or intermixed with smectite.

Quartz

Quartz is ubiquitous in the rocks beneath Pahute Mesa. It occurs as crystals and fragments in the groundmass or in lithic fragments throughout the length of the drill cores. However, in Zone 3 diagenetic quartz was noted as ~5-μm hexagonal pyramids in the groundmass, as fracture cements, and as overgrowths on phenocrysts or clasts.

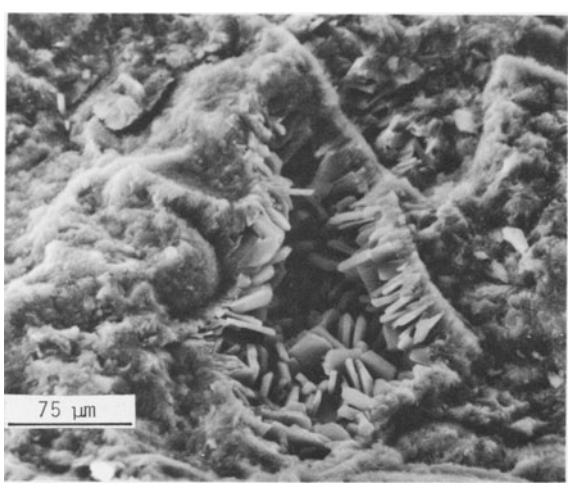

Figure 5. Scanning electron micrograph of clinoptilolite replacing glass. The rest of the field is clay.

https://doi.org/10.1346/CCMN.1981.0290508 Published online by Cambridge University Press

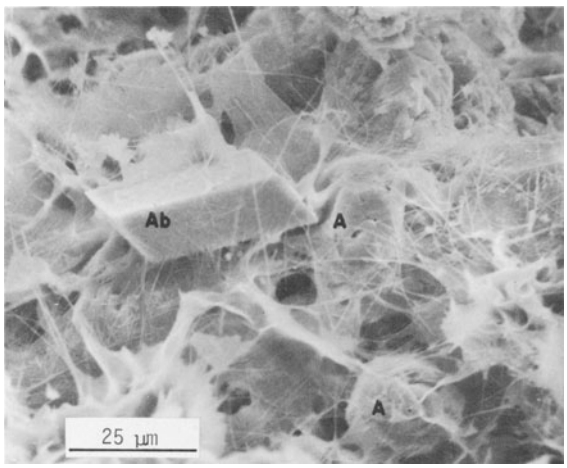

Figure 6. Scanning electron micrograph showing mordenite (M) over analcime (A) and albite (Ab).

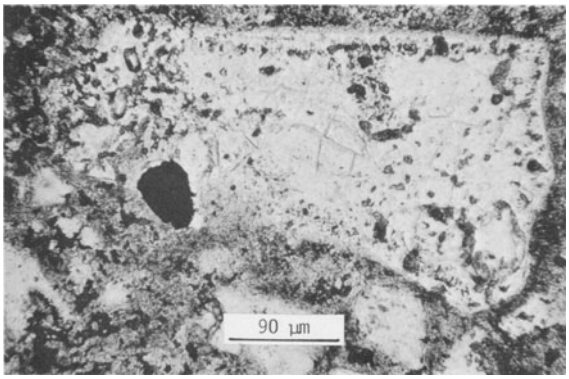

Figure 7. Photomicrograph of analcime pseudomorphous after clinoptilolite.

Authigenic feldspar

Authigenic feldspars, found in the lower parts of the cores, were identified by electron microprobe analysis and by scanning electron microscopy with multichannel X-ray analysis. Authigenic K-feldspar is common in Zone 3 and is rare in the lower parts of Zone 2. Authigenic albite is apparent only in Zone 3. It occurs as discrete, thin, bladed crystals in ghost-shard structures (at depths greater than about 1.8 km, Well UE20f), with or without K-feldspar or as alteration products of lithic fragments and plagioclase phenocrysts.

Calcite

Figure 10 shows the distribution of calcite with depth in core from Well UE20f. There is little or no calcite in Zones 1 and 2, however, it makes up an average of about 0.3% of the rock in Zone 3. Calcite fills primary pore space or is pseudomorphous after plagioclase.

CHEMICAL RESULTS

Figure 11 shows the distribution with depth of four major oxide components in Well UE20f. The oxide distributions for Wells UE20h and PM-1 are similar. These data show that the major oxides do not vary significantly with depth except between 1.0 and 1.7 km, coinciding with the distribution of mordenite in the lower part of Zone 2. With the exception of the mordenite region, there is no obvious depth control of the distribution of major elements.

The difference between the amount of inorganic carbon (in calcite) and total carbon is the amount of organic carbon (Table 4). These data indicate that there was an adequate internal supply of carbon for calcite formation.

Ground-water samples were collected and analyzed for major elements from 14 wells in Pahute Mesa by Blankennagel and Weir (1973). From these data, they reasoned that the present-day water flow is from the northeast to the southwest based on an increase in total dissolved solids from the northeastern part of the caldera southwest to the north-central Amargosa Desert.

REACTION SEQUENCES

From the mineralogical and chemical data presented above, two styles of alteration can be recognized in the rocks beneath Pahute Mesa. Hydration reactions resulted in the authigenic assemblages found in Zones 1 and 2; whereas, dehydration reactions produced most

Table 2. Partial electron-microprobe analyses of clinoptilolite.

	Wt. %			
Oxide	1	2	3	4
SiO_2	67.45	72.11	76.24	62.77
Al_2O_3	12.82	13.42	10.53	10.07
K_2O	4.64	4.73	3.69	4.83
Na_2O	3.75	3.85	2.31	2.69
CaO	0.96	1.03	0.99	0.39
Fe_2O_3	0.00	0.03	0.40	0.05

1, 2, and 3 are from Well UE20f at 0.87 km; 4 is from Well PM-1 at 0.51 km.

Table 3. Partial electron microprobe analyses of analcime.

	Wt. %				
Oxide	1	2	3	4	5
SiO_2	63.71	62.27	61.78	59.02	61.37
Al_2O_3	21.38	20.76	21.12	20.23	21.37
K_2O	0.00	0.14	0.00	0.03	0.00
Na_2O	11.99	12.12	12.39	12.10	12.61
CaO	0.00	0.08	0.02	0.11	0.00
Fe_2O_3	0.00	0.01	0.00	0.00	0.00

1 is from Well PM-1, 0.86 km; 2 and 3 are from Well UE20f, 1.22 km; and 4 and 5 are from Well UE20h, 1.56 km.

https://doi.org/10.1346/CCMN.1981.0290508 Published online by Cambridge University Press

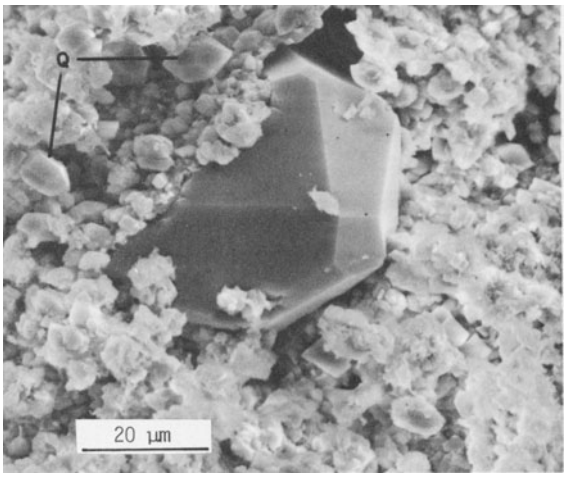

Figure 8. Scanning electron micrograph of analcime and quartz (Q).

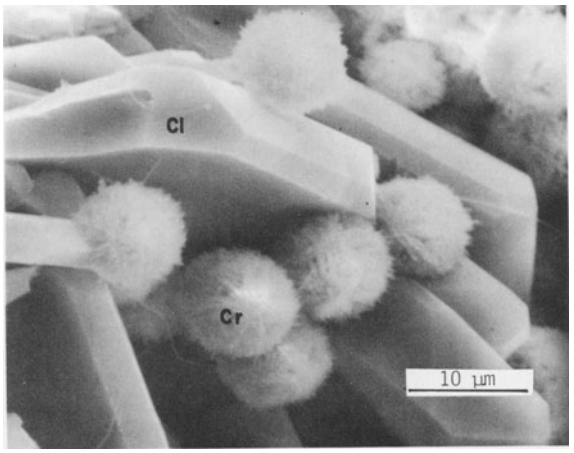

Figure 9. Scanning electron micrograph of cristobalite spherules (Cr) over clinoptilolite (Cl).

of the authigenic phases found in Zone 3. Obviously, the style of alteration is dependent on depth.

The appearance of incipient clay rims around glass shards, the formation of clinoptilolite crystals in the presence of glass and smectite, and the lack of clay domination in any sample suggest the following general hydration sequence:

$$\text{Glass} + H_2O \rightarrow \text{Smectite} + \text{Ions, and} \quad (1)$$

$$\text{Glass} + H_2O \rightarrow \text{Clinoptilolite} + \text{Ions.} \quad (2)$$

Cristobalite occurs mixed with early-formed smectite but more commonly as spherules perched on clinoptilolite. These relationships indicate that cristobalite saturation was reached during glass dissolution, yet most of the cristobalite precipitated as a late alteration product of glass. From the data in Tables 1 and 2 and the average abundances of authigenic minerals from XRD analyses, an overall reaction can be written:

$$\begin{aligned} &\text{glass} \\ &Na_{1.31}K_{1.0}Ca_{0.14}Mg_{0.04}Fe_{0.08}Al_{2.62}Si_{12.68}O_{30.7} \\ &\quad + 0.12Fe^{2+} + 0.1Ca^{2+} + 18H_2O \\ &\qquad \text{smectite} \\ &\rightarrow 0.025Na_2K_{2.4}Ca_{3.6}Mg_{1.08}Fe_{6.92}Al_{14}Si_{38}O_{100}(OH)_{20} \\ &\qquad \text{clinoptilolite} \\ &\quad + 0.981Na_{1.02}K_{0.82}Ca_{0.15}Fe_{0.03}Al_{2.16}Si_{9.84}O_{24}\cdot 8H_2O \\ &\quad + 0.26Na^+ + 0.14K^+ \\ &\qquad \text{cristobalite} \\ &\quad + 2.08SiO_2. \end{aligned} \quad (3)$$

Table 4. CO_2 analyses (Well UE20f).

Depth (km)	% CO_2 (inorg.)	% CO_2 (org.)	% CO_2 (total)
0.61	0.03	1.40	1.43
0.87	0.01	0.41	0.42
0.92	0.01	0.33	0.34
1.10	0.01	0.25	0.26
1.16	0.01	0.54	0.55
1.19	0.05	0.37	0.42
1.22	0.02	0.33	0.35
1.23	0.03	0.39	0.42
1.24	0.02	0.38	0.40
1.30	0.01	1.02	1.03
1.49	0.13	0.59	0.72
1.61	0.01	0.40	0.41
2.59	0.04	1.23	1.27
2.74	0.05	0.88	0.93
2.90	0.08	0.75	0.83
3.05	0.18	0.71	0.89
3.20	0.04	0.99	1.03
3.51	0.57	0.91	1.48
3.66	1.60	0.52	2.12
4.0	0.22	1.04	1.26

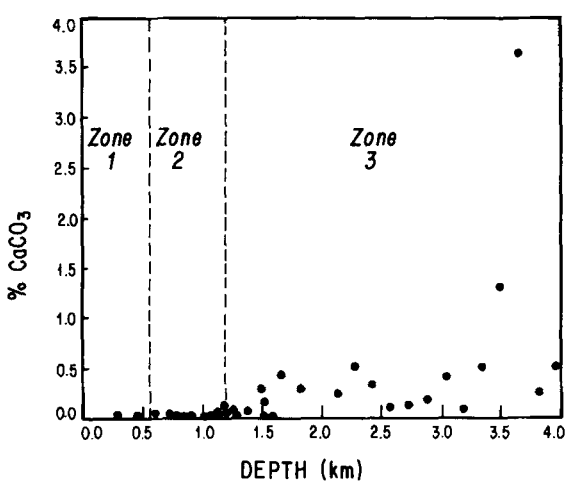

Figure 10. Plot of percent $CaCO_3$ vs. depth in Well UE20f. The sharp increase in calcite coincides with the transition from Zone 2 to Zone 3.

https://doi.org/10.1346/CCMN.1981.0290508 Published online by Cambridge University Press

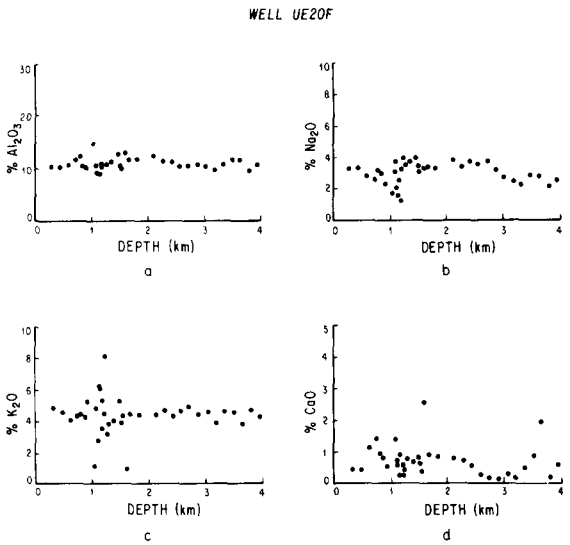

Figure 11. Plots in weight percent of (a) Al_2O_3, (b) Na_2O, (c) K_2O, and (d) CaO vs. depth in Well UE20f.

Ca^{2+} probably was immobilized within the immediate area of the dissolving glass by the relatively impermeable smectite rim as a result of its large hydration radius relative to those of monovalent cations.

Each of the products from hydration reaction (3), deep below Pahute Mesa, underwent further diagenetic change to produce the phases in Zone 3. The transition from smectite in Zone 2 to a mixed-layer illite/smectite in Zone 3 was documented by XRD analyses. The progressive increase in ordering and the decrease in expandability with depth are similar to that described by Perry and Hower (1970). This transition may be represented by the general dehydration reaction:

$$\text{Smectite} + K^+ \rightleftharpoons \text{Illite} + Na^+ + Ca^{2+} + Fe^{2+} + Mg^{2+} + SiO_2 + H_2O. \quad (4)$$

This reaction is similar to that proposed by Boles and Franks (1979) for the smectite-illite/smectite transition observed in the Tertiary pelitic sediments of the Gulf Coast.

Replacement of clinoptilolite by analcime is suggested in Figure 7. This reaction has been widely recognized in modern and ancient saline, alkaline-lake deposits (Surdam and Sheppard, 1978) as well as in other diagenetic settings (Hay, 1966). Using the data from Tables 2 and 3, the replacement of clinoptilolite by analcime may be written:

$$\underset{\text{clinoptilolite}}{Na_{1.02}K_{0.82}Ca_{0.15}Al_{2.26}Si_{9.84}O_{24}\cdot 8H_2O} + 1.14Na^+ \rightarrow \underset{\text{analcime}}{2.16NaAlSi_{2.57}O_{7.14}\cdot H_2O} + 0.15Ca^{2+} + 0.82K^+ + 4.29SiO_2 + 5.8H_2O, \quad (5)$$

where Al is conserved.

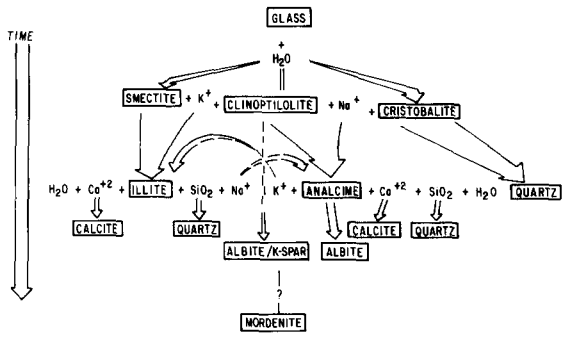

Figure 12. Summary of chronology of reactions leading to diagenetic zones.

Murata and Larson (1975) and Ernst and Calvert (1969) discussed the diagenesis of the Monterey Formation (Miocene) of California and described the transition from diatomite (amorphous silica) to cristobalite to quartz with increased depth. The silica zonation beneath Pahute Mesa is similar to the zonation in the Monterey Formation; the zones are as follows: glass (Zone 1), cristobalite (Zone 2), and quartz (Zone 3). The precipitation of quartz in Zone 3 may be represented by:

$$\underset{\text{cristobalite}}{SiO_2\cdot nH_2O} \rightarrow \underset{\text{quartz}}{SiO_2} + nH_2O, \quad (6)$$

where $n \geq 0$ depending on the degree of crystallinity of cristobalite. Quartz also probably precipitated directly from solution in Zone 3 by the reaction:

$$H_4SiO_4 \rightarrow SiO_2 + 2H_2O. \quad (7)$$

The distribution of calcite may be explained in terms of Eqs. (3–5). Eq. (3) demonstrates the dissolution of Ca^{2+} from glass and its incorporation in smectite and clinoptilolite. At depth, the Zone 2 assemblage was more unstable than at shallower depths, and smectite and clinoptilolite were replaced by illite and analcime, respectively, according to Eqs. (4) and (5). These reactions evolved Ca^{2+} which precipitated as calcite.

Figure 12 summarizes the principal reactions and relative sequences leading to the formation of Zones 1, 2, and 3. The diagram also demonstrates the interdependance of the reactions. Although absolute chronology cannot be determined, an estimate of the alteration timing has been made (*vide infra*).

The fate of feldspars is more complex and less predictable than that of the other phases. Primary plagioclase phenocrysts have undergone two different styles of progressive alteration with increased depth. The first involved the preferential dissolution along the more calcic zones and the evolution of significant intragranular secondary porosity. The second style of alteration included albitization or calcification of plagioclase in-

https://doi.org/10.1346/CCMN.1981.0290508 Published online by Cambridge University Press

volving a loss of porosity. The albitization process may be expressed as:

$$\underset{\text{anorthite}}{CaAl_2Si_2O_8} + 0.989H^+ + 1.011Na^+ + 2.023H_4SiO_4 \rightarrow \underset{\text{albite}}{1.011NaAlSi_3O_8} + \underset{\text{kaolinite}}{0.495Al_2Si_2O_5(OH)_4} + Ca^{2+} + 3.55H_2O \quad (8)$$

Eq. (8) is written to account for the volumetric replacement of calcic plagioclase by albite where Al is conserved by the formation of kaolinite. The formation of discrete authigenic albite and K-feldspar within shard outlines postdated the dissolution of clinoptilolite because the zeolite was the first to replace glass.

Chronologically, the formation of mordenite does not fit this sequence of alteration with increased depth. Mordenite fibers are found over clinoptilolite and cristobalite in Zone 2 and over analcime and albite (Figure 6) in the upper part of Zone 3. Clearly, the precipitation of mordenite postdated the formation of diagenetic Zones 1, 2, and 3.

OPEN-SYSTEM VS. CLOSED-SYSTEM DIAGENESIS

The distribution of authigenic phases beneath Pahute Mesa is similar to that of Tertiary geosynclinal deposits in the Niigata Oil Field in Japan. Here, the diagenetic mineral zonation is considered to be controlled primarily by the thermal gradient in an essentially closed hydrologic system (Iijima and Utada, 1971; Hay, 1977). However, the zeolite zonation at the Nevada Test Site previously had been correlated more closely with diagenesis in an open hydrologic system (Hoover, 1968; Hay and Sheppard, 1977). We think that there is significant evidence to show that the primary authigenic mineral zonation below Pahute Mesa was a result of closed-system burial diagenesis.

Chemical variations

From the data in Figure 11, it is apparent, with the exception of the mordenite region (about 1–1.7 km), that the variation in bulk chemistry from unaltered to highly altered rocks is insignificant. This observation implies that diagenesis did not involve significant mass transfer. However, in zeolitic rocks, dry bulk density increases about 10–15% with depth. Combining these observations, D. L. Hoover (U.S. Geological Survey, Denver, Colorado, written communication) stated that "a constant weight percent cannot be a constant content of cations when zeolitization occurs"—meaning that the increase in mass was derived from the leaching of shallower, vitric rocks and the reprecipitation of new phases at depth.

To increase mass without changing bulk chemistry by a leaching mechanism, shallow vitric rocks must dissolve in migrating waters in stoichiometric proportion similar to that of glass. Precipitation at depth must also be done stoichiometrically. We believe that highly saturated (probably supersaturated) waters could not migrate through rock having a high density of nucleation sites without changing composition. We also believe that an open-system, leaching-concentration mechanism would result in depletions or enrichments in bulk chemistry in different parts of the system (see Walton, 1975). Therefore, the absence of bulk chemical variation below Pahute Mesa suggests that diagenesis did not involve significant mass transfer. Furthermore, the increase in bulk density may be accounted for by 10–15% compaction.

Porosity and permeability

To move fluids through porous media, there must be sufficient effective porosity and permeability and a gradient or potential to initiate and maintain fluid movement. Transfer of ions through the medium is controlled by convection and diffusion. Aquifers in the present day Pahute Mesa result from fracture permeability in welded tuffs and rhyolites (Blankennagel and Weir, 1973). In contrast, the aquitards are in zeolitized rocks (Zones 1 and 2) that constitute most of the Tertiary section. Fracture permeability is minor in zeolitic rocks of Zones 2 and 3 chiefly because of their incompetence. Zone 1 (characterized by unaltered glass) is in essentially unsaturated rock. If a vertical leaching-concentration mechanism resulted in the formation of clinoptilolite (Zone 2) and finally analcime (Zone 3), an open system must have been maintained for the duration of the process. Table 5 shows porosities and permeabilities of rocks from each diagenetic zone. The extremely low permeabilities of rocks from Zones 1 and 2 imply that fluid movement was severely restricted. As indicated in Figure 5, regardless of these relatively high porosities, the pore spaces are effectively sealed.

To test this restricted fluid movement (or closed-system) hypothesis, a mathematical model for chemical mass transfer was designed using a solution to the one-dimensional, nonsteady-state, convective-diffusion equation (Gupta and Greenkorn, 1974):

$$\partial c/\partial t = D(\partial^2/\partial x^2) - V(\partial c/\partial x) \quad (10)$$

where, c = concentration, t = time, D = diffusion coefficient, V = velocity in the x direction, and x = distance in the x direction.

The initial and boundary conditions assume that: (1) $c\ (x,0) = 0$ for $x > 0$; (2) $c\ (0,t) = c$ for $t \geq 0$; (3) $c\ (\infty,t) = 0$ for $t \geq 0$; (4) $t = 10$ my (approximate age of youngest rocks); (5) $V = 5 \times 10^{-10}$ cm/sec (from measured transmissivities in the tuff aquitard (Winograd and Thordarson, 1975)); and (6) $x = 3$ km (depth below Pahute Mesa).

Assumptions (2) and (4), respectively, create an infinite reservoir (at $x = 0$) of diffusing component c, and

https://doi.org/10.1346/CCMN.1981.0290508 Published online by Cambridge University Press

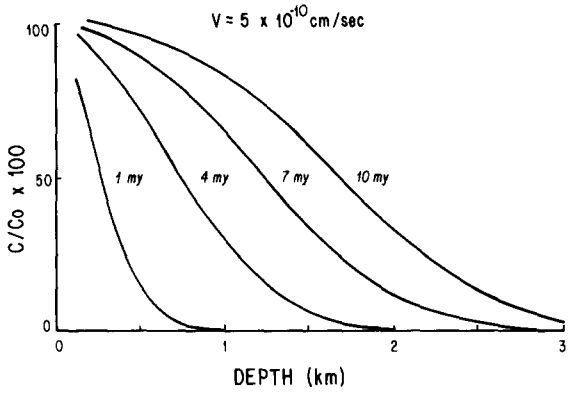

Figure 13. Convective-diffusion profiles. The concentration (C_0) of a component is held constant for all t at depth = 0. Profiles show the change in the amount of that component with depth for different t. (A diffusion coefficient of 10^{-5} cm²/sec was assumed.)

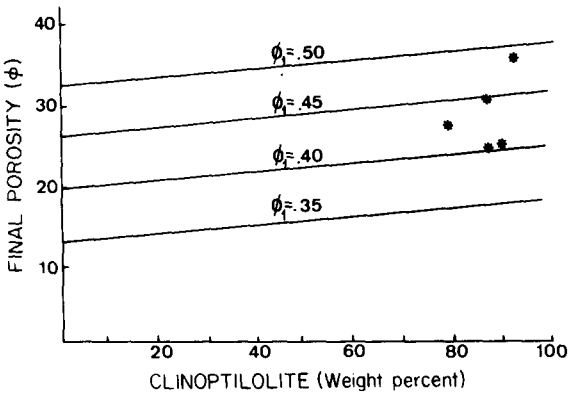

Figure 14. Plot of calculated weight percent clinoptilolite vs. final porosity for different initial porosities. Points represent measured values of percent clinoptilolite and porosity. Inferred initial porosities of 40–50% are consistent with measured values for the vitric tuffs.

give ample time for mass movement and thus provide optimum conditions for the transfer of mass. The result of this hypothetical test is shown in Figure 13 and indicates that under optimum conditions the increase in concentration of ions at depth due to convection and diffusion is minor (see 10-my curve at 3 km, Figure 13).

MASS- AND VOLUME-BALANCE CALCULATIONS

Mass- and volume-balance calculations may be utilized to test the following:

(1) From the predicted reaction sequences, do mathematically constructed mineral assemblages match the measured physical and chemical properties of the "real" assemblages?
(2) Is the addition of components to sustain a reaction consistent with a closed-system model?

Tests of this type require the following assumptions:

(1) The bulk composition of originally vitric rocks in Zones 2 and 3 were about the same as glasses in Zone 1 (for diagenetic considerations). This is consistent with the data in Table 1.
(2) The mineral compositions are assumed to be valid and representative.
(3) Reactions conserve Al. This is a valid assumption for two reasons: first, weight percent Al does not vary significantly from zone to zone; and second, at the pH and temperature range of waters below Pahute Mesa, Al mobility is probably negligible.

The mass- and volume-balanced model first utilizes Eq. (3) to produce the Zone 2 assemblage. A very small amount of smectite was first formed from glass with a given initial porosity. The residual Al was consumed to produce clinoptilolite. Cristobalite precipitated next in a quantity governed by cristobalite solubility. The final porosity was calculated from the volume of the solid phases. This calculation was repeated, each time increasing the amount of clay that was formed. Figure 14 is a plot of weight percent clinoptilolite formed vs. final porosity (ϕ_f) for the alteration of glasses with initial porosities, ϕ_i (contours). As Figure 14 illustrates, Eq. (3) involves a porosity reduction of about 15–20% depending on how much smectite is produced.

The points on Figure 14 represent measured values for typical rocks from Zone 2. These points suggest that the initial porosities of the glass precursors were 40–50%, values that are consistent with measured values for unaltered glasses (subtracting phenocryst volumes). The final porosities of 25–35%, which is again consistent with measured values, mean that these rocks underwent a porosity loss of about 15%. Even though there was a porosity reduction, to form these hydrated phases and still have saturated pore spaces, water must have been added to the system. The system can be considered closed because this water requirement is very small. Eq. (3) requires that only 0.13 pore volumes must be added to the system in order that the reaction be completed. Therefore, not only did the alteration of glass have a negligible effect on permeability (see Table 5), but the physical rearrangement of material due to the reactions did not require a higher permeability or an open system.

To summarize, the calculations adequately predict by Eq. (3) an assemblage with similar bulk chemistry, mineralogy, and porosity as that of Zone 2 rocks. Furthermore, the model is consistent with a closed-system interpretation.

Next, the model was expanded to incorporate Eqs. (4–6) to test the hypothesis pertaining to the origin of analcime, smectite/illite, calcite, and quartz. The simulated Zone 2 assemblage was used to generate the

https://doi.org/10.1346/CCMN.1981.0290508 Published online by Cambridge University Press

Zone 3 assemblage using similar methods. Depending on the actual compositions and densities, Eq. (4) increases porosity by about 1–3% (ϕ_{f1}). If Zone 2 clinoptilolite was altered by Eq. (5), precipitation of analcime, quartz, and calcite resulted in an increase in porosity of ~1% (ϕ_{f2}). The replacement of cristobalite by quartz (Eq. (6)) involves a porosity increase of ~1% (ϕ_{f3}). Therefore, the conversion of a Zone 2 assemblage to the Zone 3 assemblage involves an *increase* in porosity of 3–5% ($\phi_{f1} + \phi_{f2} + \phi_{f3}$). Unfortunately, this prediction cannot be tested accurately. Measured values show a *decreasing* trend in porosity of about 10% per kilometer, yet there is a corresponding increase in lithic content ("dead volume") with depth of ~9%, thus clouding the significance of measured porosities.

To test for an open or closed system, the amounts of Na needed to satisfy Eq. (5) and the amount of CO_3^{2-} needed to make calcite must be evaluated. Calculations show that a maximum of about 4 pore volumes of water are needed to supply the Na required by Eq. (5). This value does not account for an additional internal supply of Na from the dissolution of plagioclase or from the illitization of smectite.

The Ca in calcite reasonably matches the amount of Ca from a clinoptilolite and smectite source. If an atmospheric source of CO_2 is proposed to account for the amounts of calcite found in Zone 3, it would require a flux of as much as 10^5 pore volumes of water. This volume of water would certainly exceed closed-system requirements. However, Table 4 demonstrates that an adequate internal supply of CO_2 existed (due to the present excess of organic carbon), as a result of decarboxylation or cracking of organic compounds. These mass-balance calculations indicate that the diagenetic reactions did not require an open system with respect to fluids.

DIAGENETIC MODEL

We propose an alternate mechanism to the open-system model (Hoover, 1968) for diagenesis below Pahute Mesa for the following reasons: (1) Constant chemical composition of rocks with depth suggests that negligible mass transfer was involved in the formation of the diagenetic zones (except for the late stage precipitation of mordenite); (2) Rates of chemical mass transfer are low enough to invoke a closed-system interpretation; and (3) Mass and volume changes incurred by the diagenetic reactions satisfy closed-system requirements. The following interpretation is based on these criteria.

The initial pore-water chemistry was controlled mainly by the dissolution of highly soluble volcanic glass. As the salinity and alkalinity increased due to this dissolution, saturation with respect to various phases was attained. At greater depths, saturation was reached faster due to the accelerated rate of glass dissolution at higher temperatures. The rate at which salinity and pH increased was greater than the rate at which the first phase, smectite, precipitated. As a result, waters became supersaturated with respect to smectite and climbed rapidly into a feldspar stability field. The sluggishness with which K-feldspar or albite precipitated was overcome by the rate at which the clinoptilolite formed. The metastable precipitation of clinoptilolite exerted major controls on solution chemistry as ions were removed from solution stoichiometrically. Similarly, cristobalite precipitated metastably (instead of quartz) as a result of the kinetic barriers to rapid quartz precipitation. Thus, vitric rocks at depth were altered to a Zone 2 assemblage due to a prolonged exposure to pore waters at an elevated temperature. This process essentially conserved mass and caused no significant changes in permeability, yet porosity was reduced by as much as 15%. The process was probably occurring during the accumulation of tuffs and rhyolites in and above the Silent Canyon Caldera, and shortly after the establishment of a water table. As rocks continued to accumulate, the hydration process continued (formation of Zone 2), and the initially zeolitic rocks were progressively subjected to higher temperatures due to burial. As a result of time and temperature, the metastable hydration products underwent dehydration. Eventually, clinoptilolite was replaced by analcime and possibly K-feldspar and albite, and smectite was transformed to a mixed-layer illite/smectite having progressively decreasing expandability with depth. The release of Ca due to these reactions resulted in calcite precipitation. At these elevated temperatures, the degree of saturation with respect to quartz was lowered thus reducing kinetic barriers to quartz precipitation (Murata and Larson, 1975). As a result, quartz replaced cristobalite. Simultaneously, plagioclase suffered the effects of time and temperature and was either dissolved or albitized. With more time and greater depth of burial (temperature), analcime was replaced by albite. This second phase of alteration (formation of Zone 3) resulted in a porosity increase of as much as 5% and an increase in permeability by two or three orders of magnitude. This process also conserved mass.

The thermal conditions during diagenesis below Pahute Mesa may be inferred from other diagenetic en-

Table 5. Core plug porosities and permeabilities.

Zone	Well UE20f depth (km)	Permeability (md) Horiz.	Horiz. (90°)	Vert.	Porosity (%)
1	0.54	2429	0.03	1294	34.9
2	0.74	0.04	0.03	0.01	25.4
2	0.80	0.02	0.01	0.01	14.5
2	1.20	0.13	0.08	0.12	24.5
2–3	1.22	4.6	3.6	1.7	26.9
3	1.76	4.8	4.3	4.3	29.9
3	2.09	0.46	0.37	0.28	22.6

https://doi.org/10.1346/CCMN.1981.0290508 Published online by Cambridge University Press

vironments of similar age that underwent similar reactions. Thermal gradients from the Monterey Formation (silica reactions), the Tertiary Gulf Coast (clay mineral reactions), and the Niigata Oil Field (zeolite zonation) were readjusted for the depths below Pahute Mesa (Well UE20f) at which analogous zone boundaries occur. The calculated thermal gradient is 50°–90°C/km. The present-day thermal gradient below Pahute Mesa (Well UE20f) is 25°C/km. Inasmuch as Pahute Mesa was in a region of active heat production during and after emplacement of the tuffs, and from the analogs above, diagenetic zonation probably took place under thermal gradients significantly higher than that at present.

To summarize, the diagenetic zones below Pahute Mesa are a result of three factors: (1) changing porewater chemistry in an essentially closed hydrologic system, (2) disequilibrium precipitation, and (3) a thermal gradient that was much higher than that now present.

ACKNOWLEDGMENTS

Support for this research was provided by Lawrence Livermore National Laboratory Fund No. W-7405-ENG-48. The authors are grateful for enlightening discussions with J. I. Drever, J. R. Boles, R. C. Antweiler, and J. E. Weir.

REFERENCES

Blankennagel, R. K. and Weir, J. E. (1973) Geohydrology of the eastern part of Pahute Mesa, Nevada Test Site, Nye County, Nevada: *U.S. Geol. Surv. Prof. Pap.* **712-B,** 35 pp.

Boles, J. R. and Franks, S. G. (1979) Clay diagenesis in Wilcox Sandstones of southwest Texas: Implications of smectite diagenesis on sandstone cement: *J. Sediment. Petrol.* **49,** 55–70.

Coombs, D. S. and Whetten, J. T. (1967) Composition of analcime from sedimentary and burial metamorphic rocks: *Geol. Soc. Amer. Bull.* **78,** 269–282.

Drever, J. I. (1973) The preparation of oriented clay mineral specimens for X-ray diffraction analysis by a filter-membrane peel technique: *Amer. Mineral.* **58,** 553–554.

Ernst, W. G. and Calvert, S. E. (1969) An experimental study of the recrystallization of porcelanite and its bearing on the origin of some bedded cherts: *Amer. J. Sci.* **267-A,** 114–133.

Gupta, S. P. and Greenkorn, R. A. (1974) Determination of dispersion and nonlinear adsorption parameters for flow in porous media: *Water Resour. Res.* **10,** 839–846.

Hay, R. L. (1963) Stratigraphy and zeolite diagenesis of the John Day Formation of Oregon: *Univ. Calif. Pub. Geol. Sci.*, **42,** 199–262.

Hay, R. L. (1966) Zeolites and Zeolitic Reactions in Sedimentary Rocks: *Geol. Soc. Amer. Spec. Pap.* **85,** 130 pp.

Hay, R. L. (1977) Geology of zeolites in sedimentary rocks: in *Mineralogy and Geology of Natural Zeolites,* F. A. Mumpton, ed., Mineral. Soc. Amer. Short Course Notes **4,** 53–63.

Hay, R. L. and Sheppard, R. A. (1977) Zeolites in open hydrologic systems: in *Mineralogy and Geology of Natural Zeolites,* F. A. Mumpton, ed., Mineral. Soc. Amer. Short Course Notes **4,** 93–102.

Hoover, D. L. (1968) Genesis of zeolites, Nevada Test Site: *Geol. Soc. Amer. Mem.* **110,** 275–284.

Iijima, A. and Utada, M. (1971) Present-day zeolite diagenesis of Neogene geosynclinal deposits in the Niigata oil field, Japan: in *Molecular Sieve Zeolites*—1, Adv. Chem. Ser. **101,** *Amer. Chem. Soc.*, Washington, D.C., 548–555.

Murata, K. J. and Larson, R. R. (1975) Diagenesis of Miocene siliceous shales, Temblor Range, California: *U.S. Geol. Surv. J. Res.* **3,** 553–566.

Orkild, P. P., Byers, F. M., Jr., Hoover, D. L., and Sargent, K. A. (1968) Subsurface geology of Silent Canyon Caldera, Nevada Test Site, Nevada: *Geol. Soc. Amer. Mem.* **110,** 77–86.

Orkild, P. P., Sargent, K. A., and Snyder, R. P. (1969) Geologic map of Pahute Mesa, Nevada Test Site and vicinity, Nye County, Nevada: *U.S. Geol. Surv. Misc. Geol. Invest. Map* **I-567.**

Perry, E. and Hower, J. (1970) Burial diagenesis in Gulf Coast pelitic sediments: *Clays & Clay Minerals* **18,** 165–177.

Quinlivan, W. D. and Byers, F. M., Jr. (1977) Chemical data and variation diagrams of igneous rocks from the Timber Mountain-Oasis Valley Caldera complex, southern Nevada: *U.S. Geol. Surv. Open-File Rept.* **77-724,** 9 pp.

Ross, C. S. and Smith, R. L. (1961) Ash-flow tuffs: their origins, geologic relations, and identification: *U.S. Geol. Surv. Prof. Pap.* **366,** 81 pp.

Surdam, R. C. and Sheppard, R. A. (1978) Zeolites in saline, alkaline-lake deposits: in *Natural Zeolites: Occurrence, Properties, Use,* L. B. Sand and F. A. Mumpton, eds., Pergamon Press, Elmsford, N.Y., 145–178.

Walton, A. W. (1975) Zeolite diagenesis in Oligocene volcanic sediments, Trans-Pecos Texas: *Geol. Soc. Amer. Bull.* **86,** 615–624.

Winograd, I. J. and Thordarson, W. (1975) Hydrogeologic and hydrochemical framework, south-central Great Basin, Nevada-California, with special reference to the Nevada Test Site: *U.S. Geol. Surv. Prof. Pap.* **712-C,** 126 pp.

(Received 11 December 1980; accepted 1 June 1981).

Резюме—Тетричные кремнеземные вулканические породы в Тихом Каньоне Кальдера ниже Пагуте Меса, на месте испытаний Отдела Энергии штата Невады, были подразделены на три вертикальные минералогические зоны, с разными толщинами и нарушенными стратиграфичесдими границами. Зональные контакты являются обычно определенными. Зона 1, самая высокая зона, включает неизмененное или измененное в начальной стадии реолитическое стекло. Зона 2 характеризуется наличием преимущественно клиноптилолита и умеренного количества смектита, кристобаллита и морденита. Зона 3 характеризуется сложным минералогическим составом, который включает анальцим, кварц, кальцит, аутигенный K-фельдшпат, и альбит, каолинит, хлорит, и смешано-слойный иллит/смектит. Смешано-слойная глина выявляет увеличение упорядоченности и уменьшение способности разбухания с глубиной.

В течение короткого времени после осаждения и неглубокого погребения результатом гидратации относительно непроицаемых высоко пористых стеклянных пород было быстрое образование состава Зоны 2 исключая морденит. Результатом этой стадии перемены была потеря пористости нетто и пренебрежимо малый перенос массы. Продолжающееся погребение и всрост температуры приводили к стадии дегидратации, в которой минералы Зоны 2 были заменены минералами Зоны 3. Результатом стадии дегидратации было увеличение пористости и проницаемости на несколько порядков. Этот процесс, как и более ранние реакции, также происходил с сохранением массы. Осаждение морденита наступало после образования этого зонального состава. Диагенетические зоны ниже Пагуте Меса были результатом: (1) изменяющейся химии поровой воды в основном замкнутой гидрологической системе; (2) неравновесия или кинетического осаждения метастабильных фаз; и (3) более высокого термального градиента, присутствующего ранее. [E.C.]

Resümee—Die tertiären SiO_2-reichen vulkanischen Gesteine in der Silent Canyon Caldera unter Pahute Mesa, Department of Energy's Nevada Test Site, wurden in 3 vertikale mineralogische Zonen geteilt, die in der Dicke variieren und über stratigraphische Grenzen gehen. Die Grenzen zwischen den einzelnen Zonen sind im allgemeinen scharf. Die Zone 1, die oberste Zone, enthält unverändertes oder kaum verändertes rhyolithisches Glas. Die Zone 2 wird durch ein Vorherrschen von Klinoptilolit charakterisiert, untergeordnet treten Smektit, Cristobalit, und Mordenit auf. Die Zone 3 ist eine vielfältige Mineralvergesellschaftung, die Analcim, Quarz, Calcit, authigenen K-Feldspat, und Albit, Kaolinit, Chlorit, und Illit-Smektit-Wechsellagerungen enthält. Die Wechsellagerung zeigt mit zunehmender Tiefe eine zunehmende Ordnung und eine Abnahme der Quellfähigkeit.

Kurz nach der Ablagerung und nach einer geringen überdeckung führte die Hydratation der relativ durchlässigen, stark porösen glasigen Gesteine zu der raschen Bildung der Mineralvergesellschaftung der Zone 2 (mit Ausnahme von Mordenit). Dieses Umwandlungsstadium führte zu einer Abnahme der Porosität und zu einem vernachlässigbaren Stofftransport. Fortschreitende überdeckung und Temperaturanstieg führten zu einem Dehydratationsstadium, in dem die Mineralvergesellschaftung der Zone 2 durch die Minerale der Zone 3 ersetzt wurde. Das Dehydratationsstadium führte zu einer Porositätszunahme und einer Zunahme der Durchlässigkeit um einige Größenordnungen. Dieser Prozeß verursachte, wie auch die früheren Reaktionen, keinen Stofftransport. Nach dieser zonaren Anordnung folgt die Fällung von Mordenit. Die diagenetischen Zonen unter Pahute Mesa wurden verursacht durch: (1) Veränderungen im Chemismus des Porenwassers in einem nahezu geschlossenen hydrologischen System; (2) Ungleichgewichts- oder kinetische Fällung metastabiler Phasen, und (3) einen höheren geothermischen Gradienten als er jetzt vorhanden ist. [U.W.]

Résumé—Les roches siliciques volcaniques tertiaires dans le Silent Canyon Caldera sous Mesa Pahute, du site de tests du département d'énergie dans le Nevada ont été divisées en trois zones minéralogiques verticales qui varient en épaisseur et qui transgressent les frontières stratigraphiques. Les contacts entre zones sont généralement marquées. Zone 1, celle du dessus, comprend du verre rhyolitique soit non-altéré, soit commençant à être altéré. La zone 2 est caractérisée par une prédominance de clinoptilolite, et des quantités subordonnées de smectite, de cristobalite, et de mordénite. Zone 3 est un assemblage minéral complexe comprenant de l'analcime, du quartz, de la calcite, de la feldspath-K et de l'albite authigéniques, de la kaolinite, de la chlorite, et de l'illite/smectite à couches mélangées.

Peu après la déposition et après un enterrement peu profond, l'hydration de roches vitriques imperméables et très poreuses a résulté en la formation rapide de l'assemblage de la zone 2 (à part la mordénite). Ce stage de l'altération a résulté en une perte nette de porosité et un transfert de masse négligeable. L'enterrement prolongé et une hausse de température a mené à un stage de déshydration auquel l'assemblage de la zone 2 a été remplacé par les minéraux de la zone 3. Le stage de déshydration a résulté en un accroîssement de plusieurs ordres de grandeur de la perméabilité. Ce procédé, comme les réactions précédentes, a aussi conservé la masse. La précipitation de mordénite a suivi la formation de cette configuration zonale. Les zones diagénétiques sous Mesa Pahute ont été causées par: (1) un changement de chimie pore-eau dans un système hydrologique essentiellement fermé; (2) un déséquilibre ou la précipitation kinétique de phases métastables; et (3) un gradient thermal plus élevé qu'il ne l'est à présent. [D.J.]